

Article ID: 1003 - 6326(2005)02 - 0361 - 05

Electrochemical properties of AB₅ type hydrogen storage alloy as anode electrocatalyst of PEMFC^①

CHEN Yun(陈 昀)^{1, 2}, WANG Xin-hua(王新华)¹, CHEN Chang-pin(陈长聘)¹,
CHEN Li-xin(陈立新)¹, C. A. C. Sequeira²

(1. Department of Materials Science and Engineering, Zhejiang University,
Hangzhou 310027, China;

2. Department of Chemical Engineering, Instituto Superior Tecnico, Lisbon 1049-001, Portugal)

Abstract: The electrocatalytic properties of hydrogen storage alloy (HSA) $\text{Mn}_{13.65}\text{Co}_{0.85}\text{Al}_{0.3}\text{Mn}_{0.3}$ substituting Pt as anode electrocatalyst of PEMFC was investigated. It is found that, after being optimized, the electrocatalytic abilities of the HSA is reasonably good, the current density of the HSA anode membrane and electrode assembly (MEA) reaches 168 mA/cm^2 at 0.5 V and 232.4 mA/cm^2 at 0.2 V , and its power density reaches the maximum value of 84 mW/cm^2 . The influence of operating temperature and hydrogen pressure on the electrocatalytic behavior of HSA anode MEA is also discussed. At 60°C under $2.02 \times 10^5 \text{ Pa H}_2$, the HSA anode shows the best electrochemical properties.

Key words: MnNiCoAlMn alloy; hydrogen storage alloy; fuel cell; anode; electrochemical property

CLC number: TG 139

Document code: A

1 INTRODUCTION

In recent years, the application of the room temperature type ($< 100^\circ\text{C}$) polymer electrolyte membrane fuel cells (PEMFCs) as a primary power source in electric vehicles and portable equipments etc has received increasing attention^[1-4]. Usually in a PEMFC system, platinum is chosen as the electrode electrocatalyst, however, it results in a high-cost PEMFC system for commercialization because Pt is a high cost, source limit metal. So, looking for another new electrocatalyst is one of the focused points in the field of PEMFC's electrode materials. So far, most research works are focused on multicomponent Pt-based compounds and their preparation^[2, 4]. The studies of using hydrogen storage alloy (HSA) instead of Pt as anode electrocatalyst of a fuel cell, especially the attempt of using HSA as anode electrocatalyst of PEMFC, are seldom reported.

Rare earth based AB₅ type HSA used as negative material for nickel/metal hydride (Ni/MH) battery was characterized by good electrochemical and mechanical properties, abundant raw materials and low cost, etc^[5-8]. Previous work^[9] indicated that HSA $\text{M}_1(\text{NiCoMnCu})_5$ (M_1 : La-rich mischmetal) as an electrocatalyst of an alkaline fuel cell (AFC) anode showed a catalytic effect.

In this paper, the performance evaluation of using typical HSA $\text{Mn}_{13.65}\text{Co}_{0.85}\text{Al}_{0.3}\text{Mn}_{0.3}$ as an anode electrocatalyst of PEMFC membrane and e-

lectrode assembly (MEA) is reported. The electrochemical properties of HSA $\text{Mn}_{13.65}\text{Co}_{0.85}\text{Al}_{0.3}\text{Mn}_{0.3}$ anode MEA is investigated and the influence of operating temperature and hydrogen pressure on the electrocatalytic behavior of HSA anode is also discussed.

2 EXPERIMENTAL

The ingot of HSA with the composition of $\text{Mn}_{13.65}\text{Co}_{0.85}\text{Al}_{0.3}\text{Mn}_{0.3}$ was prepared by induction levitation melting in a water-cooled copper crucible under argon atmosphere. The purity of the raw materials Mn, Ni, Co, Al and Mn was large than 99%. The test HSAs were mechanically crushed and grounded into powders with a dimension of less than $74 \mu\text{m}$. Before the HSA was used as anode electrocatalyst, it was modified via the following steps: firstly, the powder mixture consisting of $\text{Mn}_{13.65}\text{Co}_{0.85}\text{Al}_{0.3}\text{Mn}_{0.3}$ alloy and acetylene black was filled into a vial with mass ratio of 1 : 20 of the powder to the ball, and then the vial was evacuated, filled with $3.03 \times 10^5 \text{ Pa H}_2$. The alloy was ball milled using QM -1SP Planetary Ball Mill at a rate of 225 r/min for 0.5 h. Then the ball-milled samples were submitted to chemical surface treatment by immersing the mixture in a 6 mol/L KOH + 0.01 mol/L KBH_4 solution at 80°C for 3 h; finally, the samples was chemically coated. 3% Pd layer on the surface using a coating solution consisted of PdCl_2 , NH_4Cl , HCl , $\text{NaH}_2\text{PO}_2 \cdot \text{H}_2\text{O}$ and

① Received date: 2004 - 12 - 06; Accepted date: 2005 - 01 - 18

Correspondence: CHEN Chang-pin, Professor; Tel: + 86-571-87951152; E-mail: cpchen@zju.edu.cn

ammonia.

The conventional fabrication^[10] was employed for MEA preparation. The major materials for fabricating membrane and electrode assemblies (MEAs) were as follows: platinum-dispersed carbon (Pt/C) powder with Pt content of 39% (mass fraction, Johnson-Matthey Co) and Nafion 115 membrane and 5% Nafion solution (both were produced from Du Pont Co). The electrocatalyst layer for the anode of the test MEA consisted of 0.5 g/cm² modified composite and 0.015 g/cm² of (NH₄)₂C₂O₄ for increasing the electrochemical reaction zone. All the electrocatalyst layers for the MEA cathodes contained 10 mg/cm² Pt. Hot-pressing was finally employed to assemble the anode, the cathode and membrane for the experiments. All the parts were piled up in sequence of anode gas diffusion layer, anode electrocatalyst layer, membrane cathode gas diffusion layer and cathode electrocatalyst layer. The assemblies were hot pressed for 100 s at 150–170 °C with pressure of 2.94–5.88 MPa. The whole processes were fulfilled in the presence of high purity argon.

The electrochemical measurements of the test MEAs were performed in a laboratory PEMFC cell which included a gas control loop and a thermal management loop. In the experiment, the MEA with Pt/C anode was introduced for comparison and analysis so as to evaluate the cell performance of the optimized the MEA with HSA anode. The electrochemical impedance spectroscopy (EIS) measurements for the MEA samples were fulfilled with a frequency response analyzer (1255 B) combined with Solartron SI1287 electrochemical interface driven by Zplot software. The impedance data generally covered the frequency range of 10 kHz to 5.0 mHz with 5 mV amplitude of the sinusoidal voltage. The Zview2.0 software was employed for simulation and calculation according to a given equivalent circuit.

3 RESULTS AND DISCUSSION

3.1 Cell performance of MEA with HSA anode

Fig. 1 illustrates the curves of $U-J$ and $P-J$ of the Pt/C anode MEA and the HSA anode MEA. It shows that the current densities of the HSA anode MEA reach 168 mA/cm² at 0.5 V and 232.4 mA/cm² at 0.2 V, respectively, with maximum power density of 84 mW/cm². The Tafel plots of $\ln J$ vs η shown in Fig. 2 are obtained by applying the Tafel expression, $\eta = a + b \lg J$ and the experimental data. By simulating the linear part in Tafel plots and obtaining the intercept and the slope of the line, we can calculate the Tafel slope and the exchange current densities, respectively, and the results of electrode parameters calculation are lis-

ted in Table 1. R_i is the slope of $U-J$ curves in the middle linear region which indicates the sum of all the resistances including activation resistance, electrolyte ion transfer resistance, electron transfer resistance, the contact resistance between electrode and collector and electrode resistance, etc.^[11-13]. From Table 1 it can be seen that the exchange current densities of the HSA anode MEA in the electrochemical activation region reaches 6.422×10^{-4} mA/cm². These data indicate that $\text{Mn}_{0.65}\text{Co}_{0.85}\text{Al}_{0.3}\text{Mn}_{0.3}$ alloy for replacing Pt/C as the

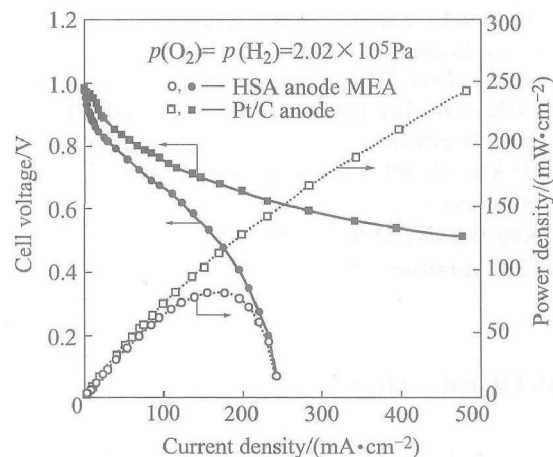


Fig. 1 Curves of $U-J$ and $P-J$ of HSA anode MEAs in comparison with Pt/C MEA at 60 °C

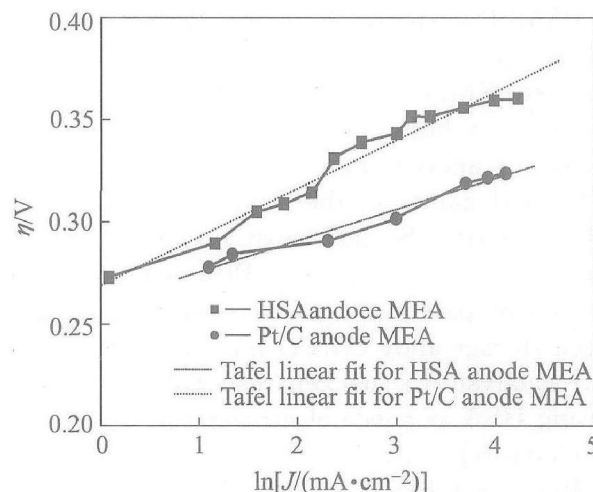


Fig. 2 Tafel plots and their linear fit of HSA anode MEA and Pt/C anode MEA

Table 1 Electrode parameters of HSA anode MEA and Pt/C anode MEA

Type of MEA	$b_{\text{Tafel}}/$ (V · dec ⁻¹)	$J_0/$ (A · cm ⁻²)	$R_i/$ (Ω · cm ⁻²)
Pt/C anode MEA	0.015 3	1.720×10^{-3}	1.57
HSA anode MEA	0.020 9	6.422×10^{-3}	2.09

Assuming cathode as MEA reaction rate limiting electrode for Pt/C MEA and assuming anode as MEA reaction rate limiting electrode for HSA anode MEA for electrode parameter calculation.

anode catalytic material shows quite good electrocatalytic abilities.

The current density of the Pt/C MEA prepared with the same method reaches 494 mA/cm² at 0.5 V, with maximum power density rising up to 247 mW/cm². Comparing Fig. 1, Fig. 2 and Table 1, we can conclude that the electrochemical properties for the MEA using Pt/C as electrode material is apparently much better than those of the HSA anode MEA. In particular, with the increase of discharge current densities, the cell voltage of the HSA anode drops rapidly, whereas the Pt/C electrode is still in higher voltage level. This is considered that, aside from the electrocatalytic properties of the materials, the existence of bigger difference is resulted from the particle size. For MEA using Pt/C as electrode material, the particle size of carbon loading Pt is 2 to 3 orders of magnitude higher than that of HSA, and such a large reaction area allows the utilization rate of Pt catalyst to be apparently higher than that of HSAs.

3.2 Effect of operating temperature on performance of HSA anode MEA

In a Pt/C fuel cell, unless the temperature rises high enough to destroy the structure of electrode or catalyst grains, cell performance is always characterized to increase with the increase of temperature, which was confirmed by most of fuel cell systems. There are several main reasons for the improvement of the properties, with higher reaction rate of electrode, all the reaction activation energy, the mass transfer resistance including electron and ion (improving the conductivity of electrolyte), and the poisoning possibility caused by impurity CO decrease.

Fig. 3 shows the effect of temperature varying on the cell performance of the HSA anode MEA, and Table 2 lists the calculated electrode parameters under four different temperatures. The results indicate that the HSA anode MEA obtained its optimum cell performance when the operating temperature is 60 °C. With the operating temperature decreasing, the electrode reaction becomes slow and the ohmic polarization increases simultaneously, and the b_{Tafel} rises from 0.020 9 V/dec at 60 °C to 0.023 4 V/dec at 30 °C and the R_i increases from 2.09 to 2.53 Ω/cm². On the other hand, when operating temperatures are 90 °C and 120 °C, the R_i values quickly go up from 2.09 at 60 °C to 7.27 and 41.5 Ω/cm², respectively, though the exchange current density (J_0) at 90 °C is 5.48×10^{-4} A/cm² and still shows a relatively high value.

Noble metal materials such as Pt and Pd. have very good hydrogen sorption plateau characteristics even at high temperature^[14]. For hydrogen storage alloys, due to its intrinsic characteristics, the equilibrium

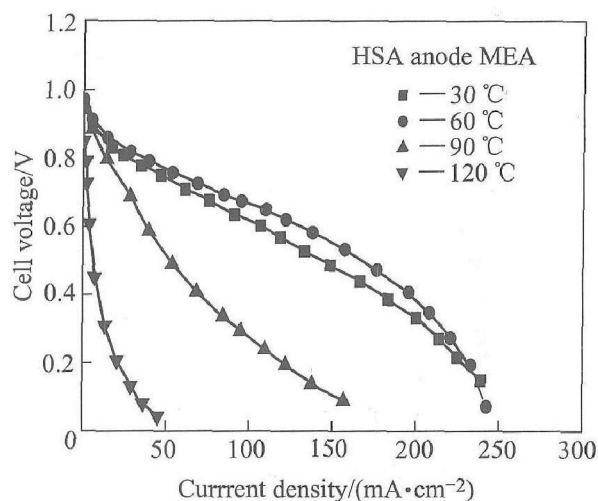


Fig. 3 Cell performance of HSA anode MEA at different temperatures

Table 2 Electrode parameters of HSA anode MEA at different temperatures (assuming anode as MEA reaction rate control electrode)

Operating temperature/ °C	$b_{Tafel}/$ (mV · dec ⁻¹)	$J_0/$ (A · cm ⁻²)	$R_i/$ (Ω · cm ⁻²)
30	23.4	1.95×10^{-4}	2.53
60	20.9	6.42×10^{-4}	2.09
90	33.4	5.48×10^{-4}	7.27
120	—	—	41.5

librium pressure was influenced greatly by the reaction temperature. The hydrogen sorption kinetics of a HSA will decrease heavily under higher temperature. The p — c — T curves of the as-cast alloy MINi_{3.65}Co_{0.85}Al_{0.3}Mn_{0.3} at different temperatures was investigated and plotted in Fig. 4. When the temperature is at 120 °C, the alloy exhibited very sloped plateau. And it can be assumed that the plateau of the alloy after 0.5 h of ball milling would become more slantwise. Under the 2.02×10^5 Pa H₂ at the same temperature, the thermodynamic hydrogen absorption content can be even lower than that of hydrogen storage alloy without ball milling. Such low hydrogen absorption capability results in fewer activated atomic hydrogen in the surface and low catalytic activities. Since the anode is in protection of reductant H₂ during the working process, it can be confirmed that the invalidation of the HSA anode was not caused by the oxidation of HSA. It is believed that under higher temperature (> 90 °C), the formation of the relatively stable phase for hydrogen catalytic sorption, i. e. metal hydride phase of MINi_{3.65}Co_{0.85}Al_{0.3}Mn_{0.3}, is very difficult, hence the rapid decrease of catalytic abilities of the anode.

3.3 EIS analysis for HSA anode MEA under different hydrogen pressure

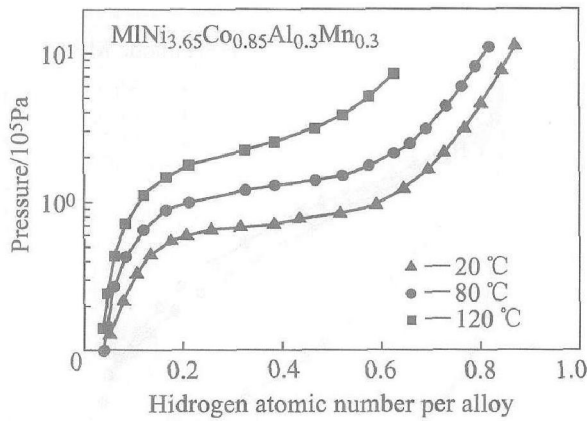


Fig. 4 p — c — T curves for HAS $\text{MINi}_{3.65}\text{Co}_{0.85}\text{Al}_{0.3}\text{Mn}_{0.3}$ at different temperatures

Fig. 5 indicates the effect of different hydrogen pressure on the charge transfer resistance R_3 of the HSA anode MEA. For HSA anode MEA, the values of R_3 are summarized in Table 3, which is used to represent the charge transfer resistances of the HSA anode due to the limit electrocatalytic abilities of HSA, are evaluated by simulating the electrochemical impedance spectroscopy as exhibited in Fig. 5 and calculated by Zview 2.0 software according to the equivalent circuit shown in Fig. 6. For comparison, the value of R_3 of Pt/C anode MEA is also listed in Table 3. However, here R_3 is considered to represent the charge transfer resistances of the Pt/C cathode because the hydrogen oxidation reaction on Pt surface is much faster than oxygen reduction reaction in Pt/C MEA.

Table 3 Charge transfer resistance R_3 of HSA anode MEA at different operating hydrogen pressures at 25 °C in comparison with Pt/C anode MEA at $p(\text{H}_2)$ 1.01×10^5 Pa

$p(\text{H}_2)/10^4$ Pa	0	1.01	5.05	10.1	20.2	10.1 (Pt/C MEA)
R_3/Ω	9.92	2.654	2.437	1.835	1.256	0.198

Generally, the electrocatalytic properties of the HSA anode MEA for hydrogen oxidation will increase with the increase of hydrogen pressure. It is exhibited in Fig. 5 that when hydrogen pressure is zero, R_3 is very large, electrode alloy is in the primary solubility range (α phase region), and electrocatalytic activities are poor; whereas with the increase of hydrogen pressure, hydrogen content in hydrogen storage alloy increases, resulting in the increase of electrocatalytic activities of the HSA electrode. This is accordant with the view of Matsuoka et al.^[15]: the electrode exchange current density will improve remarkably with the increase of hydrogen content. Within certain range, the effect of different hydrogen pressures is not appar-

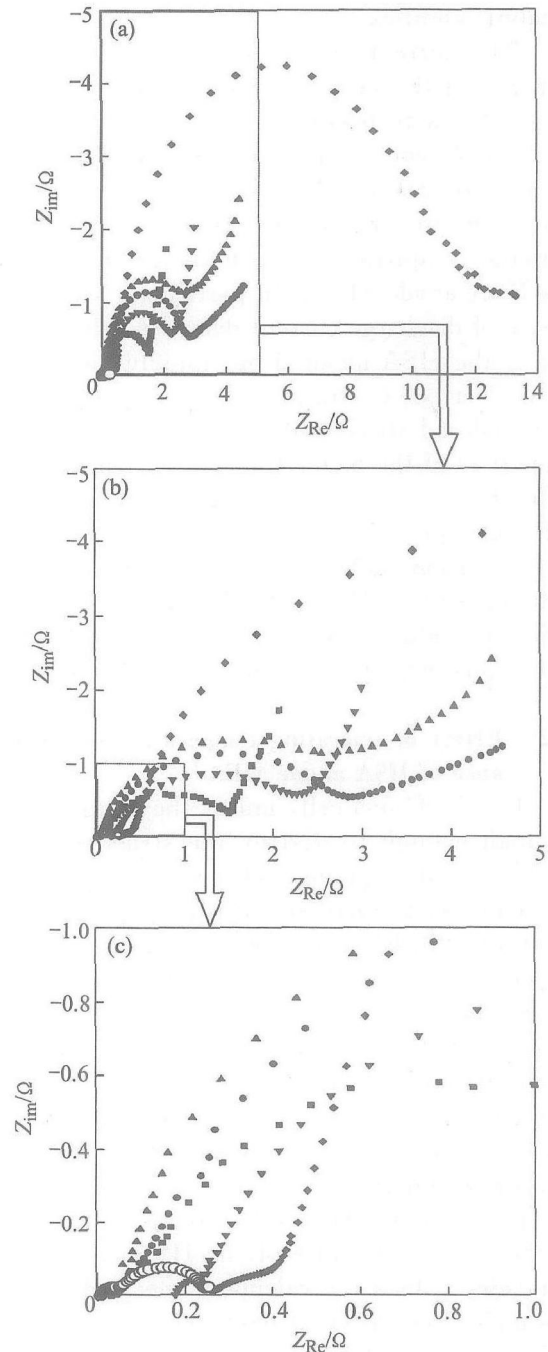


Fig. 5 Nyquist plots for HSA anode MEA at 25 °C, $p(\text{O}_2)$ 1.01×10^5 Pa and different H_2 pressures

- $-p(\text{H}_2) = 2.02 \times 10^5$ Pa; ▼ $-p(\text{H}_2) = 1.01 \times 10^5$ Pa;
- $-p(\text{H}_2) = 5.05 \times 10^4$ Pa; ▲ $-p(\text{H}_2) = 1.01 \times 10^4$ Pa;
- ◆ $-p(\text{H}_2) = 0$; ○ —Pt/C, $p(\text{H}_2) = 1.01 \times 10^5$ Pa

ent in comparing with the difference between the charge transfer resistances at 0 and 1.01×10^4 Pa. It can be explained that in the α and β phase coexisting region, the charge transfer resistances of the alloy exhibits a “plateau value”. When hydrogen pressure increases to 2.02×10^5 Pa, R_3 continues to decrease. It can be assumed that the anode HSA catalyst is still in the two phase region of $\alpha + \beta$, which indicates that increasing hydrogen pressure might further decrease the charge transfer resistance of the electrode.

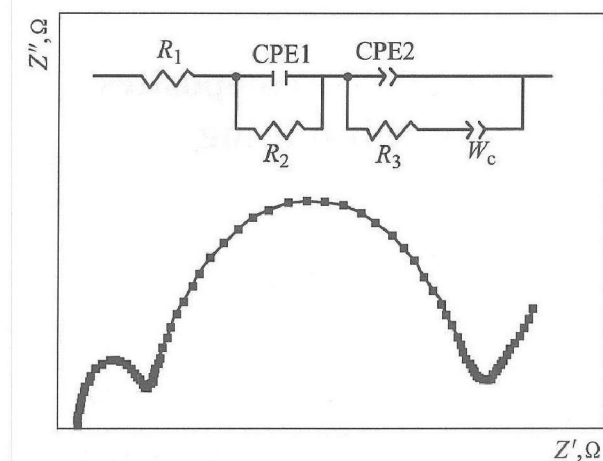


Fig. 6 Schematic images of Nyquist plot and its equivalent circuit for HSA anode MEA

4 CONCLUSIONS

1) After being optimized, the electrocatalytic abilities of the HSA $\text{M}_{1.65}\text{Ni}_{3.65}\text{Co}_{0.85}\text{Al}_{0.3}\text{Mn}_{0.3}$ is found to be reasonably good, the current density of the HSA anode MEA reaches 168 mA/cm^2 at 0.5 V and 232.4 mA/cm^2 at 0.2 V and its power density arrives the maximum value of 84 mW/cm^2 .

2) At 60°C under $p(\text{H}_2) 2.02 \times 10^5 \text{ Pa}$, the HSA anode shows the best electrocatalytic properties. The increase of operating temperature improves the electrode performance for decreasing activation polarization and ohmic polarization; however, the increase of temperature goes against the stability of metal hydride phase, resulting in the remarkable decrease of the catalytic abilities of HSA.

3) Hydrogen pressure is also one of the most important factors that affect the electrocatalytic behavior of the HSA anode. The increase of pressure enhances the electrochemical reaction rate of electrode. Within a certain range, the effect of different hydrogen pressures is not apparent in comparing with the different between the charge transfer resistances at 0 and $1.01 \times 10^5 \text{ Pa}$. It can be explained that in the α and β phase coexisting region, the charge transfer resistance of the alloy exhibits a "plateau value".

REFERENCES

[1] Ma J X, Yi B L, Yu H M, et al. Review on prepara-

tion method of membrane electrode assembly (MEA) for PEMFC [J]. Progress in Chemistry, 2004, 16(5): 804 - 812.

- [2] Rajalakshmi N, Ryu H, Dhathathreyan K S. Platinum catalyzed membranes for proton exchange membrane fuel cells - higher performance [J]. Chemical Engineering Journal, 2004, 102(3): 241 - 247.
- [3] Williams M V, Begg E, Bonville L, et al. Characterization of gas diffusion layers for PEMFC [J]. J Electrochem Soc, 2004, 151(8): A1173 - A1180.
- [4] Li Y H, Chen J F, Ding J, et al. Effect of Pt/Ru supported by carbon nanotubes on the ability of PEMFC to resist CO poisoning [J]. J Inorg Mat, 2004, 19(3): 629 - 633.
- [5] Fukunaga H, Yang H B, Matsumoto N, et al. Metal hydride electrodes using new substrates for high power applications [J]. Electrochemistry, 2004, 72(7): 503 - 507.
- [6] Shu K Y, Zhang S K, Lei Y Q, et al. Relationship between cooling rate and electrochemical performance of melt-spun AB(5) alloy [J]. Trans Nonferrous Met Soc China, 2003, 13(4): 922 - 925.
- [7] Xu Y H, Chen C P, Wang X L, et al. The analysis of the two discharge plateaus for Ti-Ni-based metal hydride electrode alloys [J]. J Power Sources, 2002, 112(1): 105 - 108.
- [8] Wang Q D, Chen C P, Lei Y Q. The recent research, development and industrial applications of metal hydrides in the People's Republic of China [J]. J Alloys Comp, 1997, 253: 629 - 635.
- [9] Wang X H, Chen, Y, Pan H G, et al. Electrochemical properties of $\text{M}_1(\text{NiCoMnCu})_5$ used as an alkaline fuel cell anode [J]. J Alloys Comp, 1999, 193 - 295: 833 - 837.
- [10] Chun Y G, Kim C S, Peck D H, et al. Performance of a polymer electrolyte membrane fuel cell with thin film catalyst electrodes [J]. J Power Sources, 1998, 71: 174 - 178.
- [11] Ticianelli E A, Rerouin C R, Redonda A. Methods to advance technology of proton exchange membrane fuel cells [J]. J Electrochem Soc, 1988, 135(9): 2209 - 2014.
- [12] Srinivasan S, Ticianelli E A, Rerouin C R. Advances in solid polymer electrolyte fuel cell technology with low platinum loading electrodes [J]. J Power Sources, 1988, 22: 359 - 375.
- [13] Kumar G, Raja M, Parthasarathy S. High performance electrodes with very low platinum loading for polymer electrolyte fuel cells [J]. Electrochim Acta, 1995, 40(3): 285 - 290.
- [14] Lewis FA. Hydrogen in palladium and palladium alloys [J]. Inter J Hydrogen Energy, 1996, 21(6): 461 - 464.
- [15] Matsuoka M, Terashima M, Iwakura C. Effect of alloy composition on charge and discharge characteristics of the negative electrode for nickel-hydrogen batteries [J]. Electrochimica Acta, 1993, 38(8): 1087 - 1092.

(Edited by LONG Huai-zhong)